

Optimization of optical parameters of an IR Fabry–Perot interferometer-based gas analyzer for carbon monoxide

A.A. Azbukin, M.A. Buldakov, B.V. Korolev,
V.A. Korol'kov, I.I. Matrosov and A.A. Tikhomirov

*Institute of Monitoring of Climatic and Ecological Systems,
Siberian Branch of the Russian Academy of Sciences, Tomsk*

Received July 31, 2006

The design of a stationary absorption gas analyzer, employing a broadband IR radiation source, an interference filter, and a Fabry–Perot interferometer, is considered. The gas analyzer is intended for measuring the concentration of CO molecules in effluent gases of heat and power plants. The optimal optical parameters of the interference filter and Fabry–Perot interferometer are calculated. It is shown that with the optimal parameters of the filter and interferometer the differential absorption signal increases by 50 to 100 times in comparison with the standard scheme of formation of the differential absorption signal without a Fabry–Perot interferometer.

Introduction

Nowadays the main anthropogenic gases: nitrogen oxides, sulfur dioxide, and carbon monoxide, are to be necessarily monitored in smoke emissions of heat and power plants for ecological purposes. The amount of gases and the smoke composition depend, to a significant degree, on the fuel used and the burning conditions. The continuous monitoring of the oxide emissions and their decrease are the main tasks of the environmental activity in the heat and power engineering, which are accomplished with the use of stationary automatic continuously operated gas analyzers. In this situation, of undoubted interest is the development of reliable and relatively cheap automatic continuously operating gas analyzers as a part of the equipment of the existing and new heat and power plants.

The Laboratory of Ecological Instrument Making at IMCES SB RAS has already developed DOG-1 and DOG-4 stationary automatic gas analyzers^{1–3} for continuous measurements of the content of nitrogen monoxide and sulfur dioxide in effluent smokes of heat and power plants. The principle of operation of these gas analyzers is the differential absorption in the near-UV spectral region ($\sim 0.23 \mu\text{m}$). The DOG-1 gas analyzer is included in the State Registry of Measurement Tools of the RF, and more than 70 such analyzers are installed at all large heat and power plants, running on the natural gas, in Tyumen' Region. The DOG-4 gas analyzer has passed the nine-month inprocess testing in 2003–2004 at Tomsk GRES-2 electric power plant and is ready for certification.

This paper presents the results of the development of a stationary automatic gas analyzer for continuous monitoring of the carbon monoxide (CO) content in the effluent smokes of heat and power plants.

Principle of operating of the Fabry–Perot interferometer-based IR gas analyzer for carbon monoxide

A characteristic feature of the CO molecule is the absence of strong absorption bands in the visible and near-UV spectral regions. In the IR region, the CO molecule possesses strong absorption in the range of the fundamental rotational-vibrational band ($\lambda \approx 4.67 \mu\text{m}$) and much weaker absorption in the overtone rotational-vibrational bands ($\lambda \approx 2.35, 1.57, \text{ and } 1.19 \mu\text{m}$) (see Ref. 4). In addition, the CO molecule has the pure rotational absorption spectrum, lying in the far-IR ($\lambda \approx 2600 \mu\text{m}$) spectral region, which is not usually used for gas analysis.

The absorption spectrum of the CO molecule in the range of the strongest IR absorption ($\lambda \approx 4.67 \mu\text{m}$) consists of two systems of rotational lines (*P*- and *R*-branches of the fundamental vibrational band), whose wave numbers (in cm^{-1}) are determined as⁵:

$$\omega_P(J) = 2143.272 - 3.862J - 0.0175J(J-2) + 0.0000245J^3, \quad (1)$$

$$\omega_R(J) = 2143.272 + 3.862(J+1) - 0.0175(J+1)(J+3) - 0.0000245(J+1)^3,$$

where J is the rotational quantum number, $J = 1, 2, 3, \dots$ for the lines of the *P*-branch and $J = 0, 1, 2, \dots$ for the lines of the *R*-branch. The difference between wave numbers of neighboring lines amounts to $\sim 3.9 \text{ cm}^{-1}$ and slightly decreases toward higher frequencies. The absorption spectrum of the CO molecule is shown in Fig. 1.

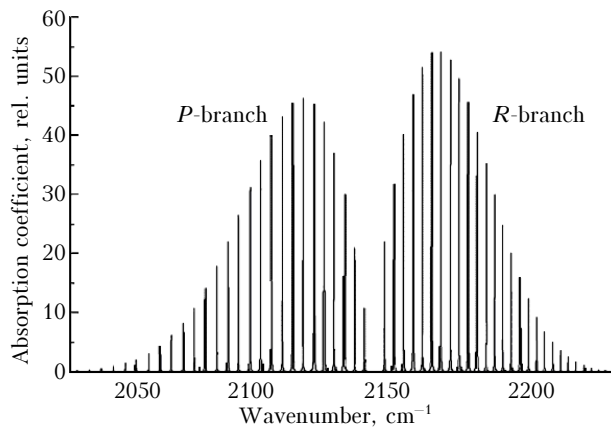


Fig. 1. Absorption spectrum of the CO molecule in the range of the fundamental rotational-vibrational band ($\lambda \approx 4.67 \mu\text{m}$) at a temperature of 300 K and pressure of 1 atm.

It is seen clearly that the IR spectrum looks like a system of nearly equidistant (in the wavenumber) spectral lines, and the half-widths of the spectral lines ($\sim 0.1 \text{ cm}^{-1}$ at the atmospheric pressure) are much smaller than the wavenumber difference between neighboring lines.

By this reason, the version of the differential absorption method, employed in the DOG-1 and DOG-4 gas analyzers, turns out to be inefficient, because the differential absorption signal

$$S = (I_1 - I_2)/I_1, \quad (2)$$

where I_2 is the intensity of the light flux passed through a gaseous medium nearby an absorption band of the gas under study and I_1 is the intensity of the light flux outside this band, weakly depends on the concentration of the absorbing molecules. This is connected with the fact that the most part of the IR radiation in the range of the absorption band (I_2) will pass through the smoke gas regardless of the content of the CO molecules in it.

In this situation, to create the IR gas analyzer for carbon monoxide, it is worth designing a specialized radiation source, with the spectrum better matched with the spectrum of the CO molecule. Such a specialized radiation source includes a source of the IR radiation with a continuous spectrum, an interference filter (IF), and a Fabry–Perot interferometer (FPI). In this design, IF and FPI form a multiband IR filter with frequency-tunable passbands, in which IF separates the radiation in the range of the CO absorption band from the continuous spectrum of the source, and FPI transmits only a set of narrow equidistant (on the wave numbers scale) spectral parts. By tuning properly the spacing between FPI plates one can make these spectral parts to coincide, in wave numbers, with the absorption lines of carbon monoxide (Fig. 2a).

In this case, the radiation is absorbed by the CO molecules (I_2 signal). If the interferometer is tilted at a small angle, its transmission peaks are shifted with respect to the CO absorption lines (Fig. 2b) and there is no radiation absorption by the CO molecules

(signal I_1). Such a specialized radiation source allows one to exclude noninformative parts of the spectrum and obtain the differential absorption caused by a number of CO absorption lines simultaneously. This circumstance is connected with the fact that the lines in the CO absorption spectrum are not exactly equidistant due to nonlinear terms present in Eqs. (1), while the FPI spectrum is exactly equidistant.

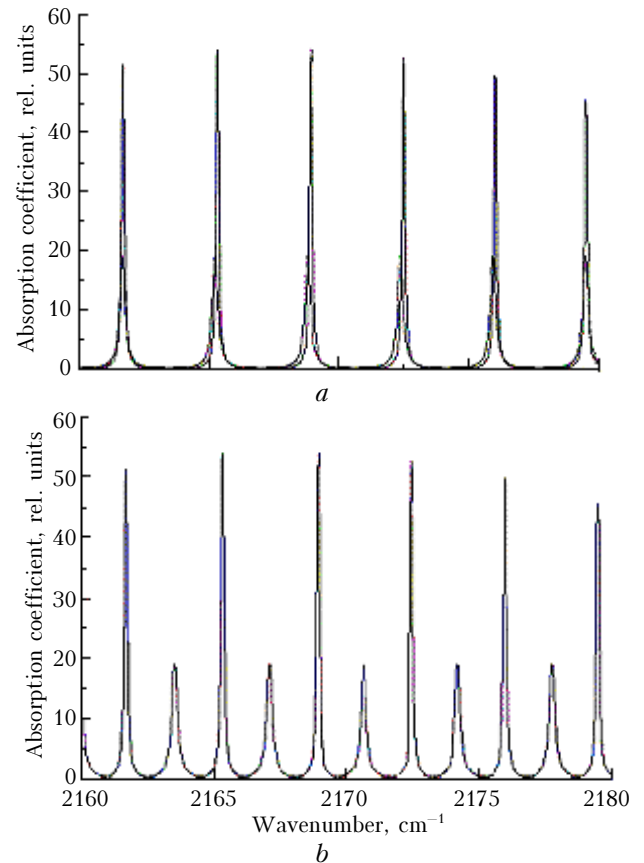


Fig. 2. Fragment of the absorption spectrum of the CO molecule in the range of the R-branch of its fundamental vibrational band: in the case that the peaks of the FPI transmission peaks coinciding with the CO absorption lines (a); in the case that the peaks of the FPI passbands are shifted with respect to the CO absorption lines (b).

Optimization of optical parameters of the CO gas analyzer

The block diagram of the prototype CO gas analyzer on the basis of a multiband IR filter is shown in Fig. 3. The photodetector signal can be presented in the form

$$I(\omega_0, \Delta\omega, R, d, T, P, l, \theta) = C \int f_{IF}(\omega_0, \Delta\omega, \omega) f_{FPI}(R, d, \omega, \theta) \times \exp[-k(T, P, \omega)Pl] d\omega, \quad (3)$$

where ω_0 and $\Delta\omega$ are the position of the peak and the half-width of the IF passband; d and R are the spacing between FPI plates and the reflection coefficient of the

FPI mirrors; θ is the FPI tilt angle; T and P are the gas temperature and pressure; l is the cell length; $f_{IF}(\omega_0, \Delta\omega, \omega)$ is the spectral density of the IF transmittance; $f_{FPI}(R, d, \omega, \theta)$ is the spectral density of the FPI transmittance; $k(T, P, \omega)$ is the spectral density of the absorption coefficient of the CO molecules at the gas temperature T and pressure P .

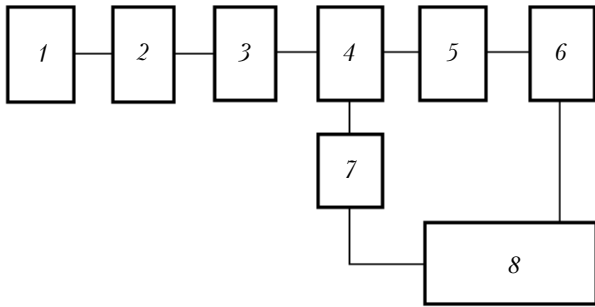


Fig. 3. Block-diagram of the prototype CO gas analyzer: IR radiation source (heated tungsten filament in the inert medium) with a modulator 1; mirror optical system 2; interference filter 3; Fabry–Perot interferometer 4; cell (with an inlet and outlet for the smoke gas) 5; photodetector 6; tilt drive for the Fabry–Perot interferometer 7; control system 8.

The spectral power of the source radiation and the spectral sensitivity of the photodetector within the CO absorption band are assumed constant and included in the coefficient C , describing the non-dispersion part of the transmission function of the gas analyzer.

With the allowance for Eq. (3), the differential absorption signal (2) in this gas analyzer can be written as

$$S(\omega_0, \Delta\omega, R, d, T, P, l, \theta) = \frac{I_1(\omega_0, \Delta\omega, R, d, T, P, l, \theta_1) - I_2(\omega_0, \Delta\omega, R, d, T, P, l, \theta_2)}{I_1(\omega_0, \Delta\omega, R, d, T, P, l, \theta_1)}, \quad (4)$$

where θ_2 is the FPI tilt angle, at which the FPI passbands coincide with the carbon monoxide absorption lines (see Fig. 2a), while θ_1 is the FPI tilt angle, at which FPI passbands lie between the carbon monoxide absorption lines (see Fig. 2b).

The maximum sensitivity of the gas analyzer on the basis of a multiband filter can be achieved only at the optimal IF and FPI parameters. The optimal parameters are understood here as the parameters, at which the differential absorption signal reaches its maximum value. The following FPI parameters should be optimized: the spacing between the FPI mirrors d and the reflection coefficients of the FPI mirrors R . Figure 4 depicts the photodetector signal (see Eq. (3)) as a function of the FPI plates separation in the range of the maximum modulation of the signal.

In the calculations, the spectral density of the FPI transmittance was presented by the Airy function⁶:

$$f_{FPI}(R, d, \omega, \theta) = \frac{(1 - R - \varepsilon)^2}{(1 - R)^2 + 4R \sin^2(2\pi d \omega \cos \theta)}, \quad (5)$$

where ε is the absorption coefficient of the mirrors (hereinafter $\varepsilon = 0.02$), and the spectral density of the IF transmittance is

$$f_{IF}(\omega_0, \Delta\omega, \omega) = \left[\frac{(1.15\Delta\omega)^2}{(\omega_0 - \omega)^2 + (1.15\Delta\omega)^2} \right]^4. \quad (6)$$

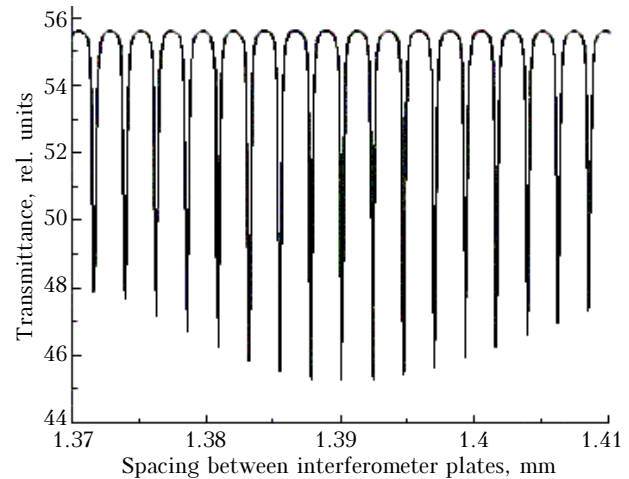


Fig. 4. Photodetector signal as a function of the FPI plate separation at $\omega_0 = 2170 \text{ cm}^{-1}$; $\Delta\omega = 15 \text{ cm}^{-1}$; $T = 300 \text{ K}$; $l = 1 \text{ cm}$; $\theta = 0^\circ$ at $R = 0.8$, and the number concentration of CO molecules $N = 10000 \text{ ppm}$.

The spectral density of the absorption coefficient of the CO molecules $k(T, P, \omega)$ was calculated by the standard technique, described in Ref. 7. The sharp dips in the signal (interference orders) in Fig. 4 correspond to the situation that the CO absorption spectrum coincides with the FPI transmission spectrum. It is clearly seen that the maximum modulation of the signal and, consequently, the maximum differential absorption signal are achieved at the FPI plate separation $d \approx 1.39 \text{ mm}$, which corresponds to the distances between the lines in the vicinity of the maximum of the CO absorption in the R -branch. The differential absorption signal as a function of the number concentration of the CO molecules is shown in Fig. 5.

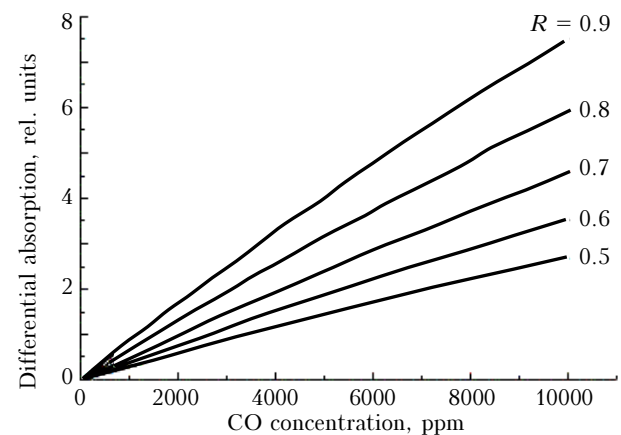


Fig. 5. Differential absorption signal as a function of the number concentration of CO molecules at the different reflection coefficients of the FPI mirrors at $\omega_0 = 2170 \text{ cm}^{-1}$; $\Delta\omega = 15 \text{ cm}^{-1}$; $T = 300 \text{ K}$; $l = 1 \text{ cm}$; $d = 1.39 \text{ mm}$.

The figure shows that at the considered concentrations of the CO molecules the differential absorption signal increases with increasing R . On the other hand, as R increases, the FPI transmittance

$$t = (1 - R - \epsilon)^2 / (1 - R)^2 \quad (7)$$

decreases, which leads to the undesirable decrease of the photodetector signals (Fig. 6).

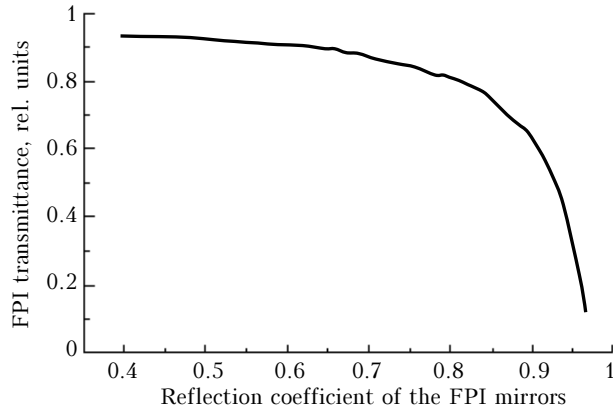


Fig. 6. FPI transmittance (at the band maximum) at the different reflection coefficients of the FPI mirrors ($\epsilon = 0.02$).

As is seen from the functions shown in Figs. 5 and 6, the optimal value of the reflection coefficient of the FPI mirrors should be taken as $R = 0.80$ – 0.85 . At such reflection coefficients, the FPI contrast

$$\gamma = \frac{f_{\text{FPI}}^{\text{max}}}{f_{\text{FPI}}^{\text{min}}} = \left(\frac{1 + R}{1 - R} \right)^2, \quad (8)$$

where $f_{\text{FPI}}^{\text{max}}$ is the spectral density at the maximum FPI transmittance and $f_{\text{FPI}}^{\text{min}}$ is the spectral density at the minimum FPI transmittance, is still high enough and equals to $\gamma \approx 100$.

For the interference filter, it is necessary to optimize the position of the maximum transmittance and the half-width of the passband. Figure 7 shows the differential absorption signal as a function of the position of the peak of the IF passband.

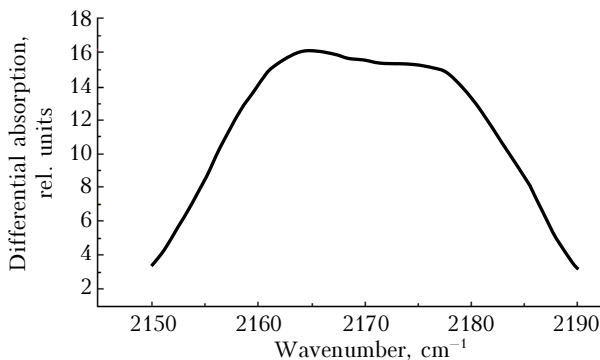


Fig. 7. Differential absorption signal as a function of the position of the peak of the IF passband at $\Delta\omega = 15 \text{ cm}^{-1}$; $T = 300 \text{ K}$; $l = 1 \text{ cm}$; $R = 0.8$; $d = 1.39 \text{ mm}$, and $N = 100 \text{ ppm}$.

The curve obtained has a wide maximum in the vicinity of the lines of the CO R -branch with the maximal absorption. This allows us to consider any value in the range of 2160 – 2180 cm^{-1} as the optimal value of the peak of the IF passband. The differential absorption signal as a function of the spectral half-width of the IF passband for two concentrations of the CO molecules is shown in Fig. 8.

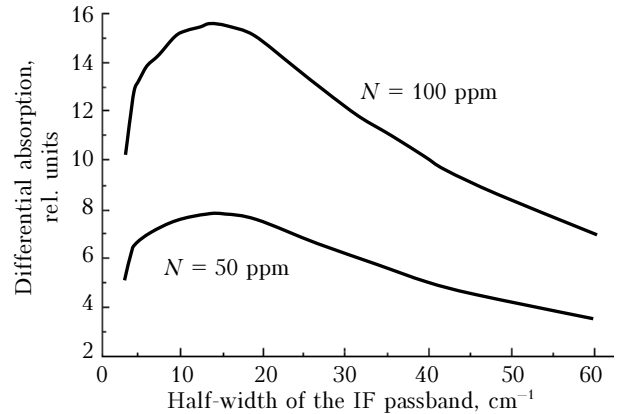


Fig. 8. Differential absorption signal as a function of the spectral half-width of the IF passband for two concentrations of the CO molecules at $\omega_0 = 2170 \text{ cm}^{-1}$; $d = 1.39 \text{ mm}$; $R = 0.8$; $T = 300 \text{ K}$; $l = 1 \text{ cm}$.

It is clearly seen that for both concentrations of the CO molecules the differential absorption signal has a peak at $\Delta\omega = 15 \text{ cm}^{-1}$. Similar behavior of the differential absorption signal is also observed for other number concentrations of the CO molecules. Thus, the results presented show that, at the optimal values of the FPI and IF parameters, only five to six most intense lines of the R -branch of the CO absorption spectrum take part simultaneously in the differential absorption.

The differential absorption signal as a function of the number concentration of the CO molecules is illustrated in Fig. 9.

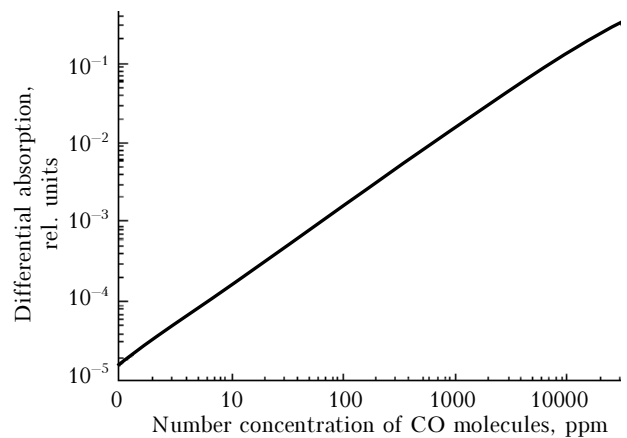


Fig. 9. Differential absorption signal as a function of the number concentration of CO molecules at the optimal FPI and IF parameters.

One can see that the dependence of the differential absorption signal on the concentration of the CO molecules remains linear up to $N \approx 10000$ ppm, which considerably exceeds the content of the CO molecules in the smoke gases of heat and power plants.

Conclusions

The calculations of the optimal parameters of the Fabry–Perot interferometer and the interference filter for the absorption IR gas analyzer for CO on the basis of a multiband IR filter have shown that the differential absorption signal at the optimal parameters increases by 50 to 100 times as compared to the standard scheme of formation of the differential absorption signal.

Acknowledgments

This study was accomplished within the framework of the SB RAS Project No. 28.2.3 “Development of New Methods, Technologies, and Instruments on the Basis of Optical, Radio-Wave, and Acoustic Effects for Monitoring of the Environmental and Anthropogenic

Systems, as well as for Solution of Specialized Problems.”

References

1. M.A. Buldakov, I.I. Ippolitov, B.V. Korolev, V.E. Lobetskii, and I.I. Matrosov, “Gas analyzer,” Patent No. 2029288 of the Russian Federation, MKI³ G 01 No. 21/61 Bull. Izobr. No. 5 (1995).
2. A.A. Azbukin, M.A. Buldakov, V.V. Zanin, B.V. Korolev, V.A. Korol’kov, and I.I. Matrosov, “Two-component optical gas analyzer,” Patent No. 2244291 of the Russian Federation, MPK⁷ G 01 N 21/61, Bull. Izobr. No.1 (2005).
3. A.A. Azbukin, M.A. Buldakov, B.V. Korolev, V.A. Korol’kov, and I.I. Matrosov, Atmos. Oceanic Opt. **15**, No. 1, 74–77 (2002).
4. G. Herzberg, *Molecular Spectra and Molecular Structure. I. Spectra of Diatomic Molecules* (Van Nostrand Reinhold, New York, 1950), 658 pp.
5. K.P. Hüber and G. Herzberg, *Constants of Diatomic Molecules* (Van Nostrand-Reinhold, New York, 1979).
6. A.N. Zaidel’, G.V. Ostrovskaia, and Yu.I. Ostrovskii, *Technology and Practice of Spectroscopy* (Nauka, Moscow, 1972), 376 pp.
7. S.S. Penner, *Quantitative Molecular Spectroscopy and Gas Emissivities* (Addison-Wesley, Reading, MA, 1959).